

# Deracemization of Bilirubin as the Marker of the Chirality of Micellar Aggregates

ALESSANDRO SORRENTI,<sup>1</sup> BARBARA ALTIERI,<sup>2</sup> FRANCESCA CECCACCI,<sup>2</sup> PIETRO DI PROFIO,<sup>3,4</sup> RAIMONDO GERMANI,<sup>3,4</sup> LUISA GIANSAANTI,<sup>1</sup> GIANFRANCO SAVELLI,<sup>3,4</sup> AND GIOVANNA MANCINI<sup>1,4\*</sup>

<sup>1</sup>CNR, Istituto di Metodologie Chimiche, Sezione Meccanismi di Reazione and Dipartimento di Chimica, Università degli Studi di Roma "La Sapienza," P.le A Moro 5, Roma, Italy

<sup>2</sup>Dipartimento di Chimica, Università degli Studi di Roma "La Sapienza," P.le A Moro 5, Roma, Italy

<sup>3</sup>Dipartimento di Chimica, Università degli Studi di Perugia, Via Elce di Sotto 8, Perugia, Italy

<sup>4</sup>Centro di Eccellenza Materiali Innovativi Nanostrutturati per Applicazioni Chimiche, Fisiche e Biomediche (CEMIN), Università degli Studi di Perugia, Via Elce di Sotto 8, Perugia, Italy

**ABSTRACT** The deracemization of bilirubin in micellar aggregates of structurally correlated chiral surfactants was studied by circular dichroism experiments and exploited as the marker of the expression of chirality of the aggregates. The obtained results suggest that the hydrophobic interactions control the transfer of chirality from the monomers to the aggregates, and that different regions of the same aggregate might feature opposite enantio-recognition capabilities. *Chirality* 24:78–85, 2012. © 2011 Wiley Periodicals, Inc.

**KEY WORDS:** circular dichroism; micelle; aggregation; deracemization; bilirubin

## INTRODUCTION

The lack of chiral symmetry is a widespread feature of nature observed at each level of complexity, from the subatomic and molecular scale to the macroscopic length scale of some living organisms. Chiral homogeneity is also a trait of the components of biological membranes, lipids and proteins, that determine and control a number of complex biological functions by self-organizing into the membrane lipid bilayers according to the program encoded in their molecular structure. As a facet of the molecular structure, chirality affects the organization and functions of biomembranes through chiral recognition and diastereomeric interactions. However, it is still poorly understood how the chiral information encoded in the monomers is transferred into the assembly and how the chiral function is translated in these complex systems.

Because of the complexity of biomembranes, many investigations, aimed at clarifying how chiral recognition works in these systems, have been carried out on models such as micelles,<sup>1–9</sup> liposomes,<sup>10–12</sup> and Langmuir monolayers.<sup>13–17</sup> Micelles, although different from biological membranes in their morphology and thermodynamics, are controlled by the same type of noncovalent interactions that control the organization of biological membrane; further, differently from lipid monolayers and bilayers they are stable and because of their small size are more suitable than other models for spectroscopic investigations. Some investigations on chiral recognition in micellar aggregates have shown that the stereochemical information of chirality may influence the morphology and the stability of the aggregates<sup>18,19</sup> and may govern the enantiodiscrimination in the interaction of chiral self-assemblies with chiral solutes.<sup>10,15,20,21</sup> Nevertheless, the mechanisms of chiral recognition and the sites of recognition in the assembly have not been completely clarified yet.

Herein, a circular dichroism (CD) investigation on the chiral recognition of bilirubin-IX $\alpha$  in micelles formed by the chiral cationic surfactants **1–4** (Scheme 1) is reported. It is known that bilirubin is a racemic mixture of conformational

enantiomers (Scheme 1) interconverting with a barrier of 18–20 kcal mol<sup>-1</sup>.<sup>22</sup> A shift of the 1:1 enantiomeric equilibrium toward one of the enantiomers has been observed in the presence of chiral selectors such as proteins,<sup>23–26</sup> chiral amines,<sup>27</sup> cyclodextrins,<sup>28</sup> and chiral micelles,<sup>29</sup> due to the different stability of the diastereomeric complexes.

In a previous investigation, it was observed that the micellar aggregates formed by the enantiopure *N*-alkyl-*N,N*-dimethyl-*N*-(1-phenylethyl)ammonium bromides are able to induce a deracemization of bilirubin racemic mixture.<sup>30</sup> Interestingly, the extent and the direction of the observed deracemization was shown to depend strongly on the length of the hydrophobic alkyl chain and on concentration conditions.

The work described here extended the above-mentioned investigation to the aggregates formed by the structurally correlated chiral cationic surfactants **1–4**, exploring how different molecular features can influence the organization of micellar aggregates and hence their expression of chirality.

## MATERIALS AND METHODS

Chemicals (Sigma-Aldrich) were of the highest grade available and were used without further purification. Solvents for the spectroscopic studies were of spectroscopic grade and used as received. Thin Layer Chromatography (TLC): Merck silica gel 60 F254; CC: Merck silica gel 60, 70–230 mesh American Society for Testing and Materials (ASTM).

<sup>1</sup>H Nuclear Magnetic Resonance (NMR) spectra were recorded on a Bruker AC 300 operating at 300.13 and 75.47 MHz for <sup>1</sup>H and <sup>13</sup>C, respectively, equipped with a sample tube thermostating apparatus. Signals were referenced with respect to tetramethylsilane (TMS) ( $\delta = 0.000$  ppm).

CD spectra were recorded on a Jasco spectropolarimeter J-715.

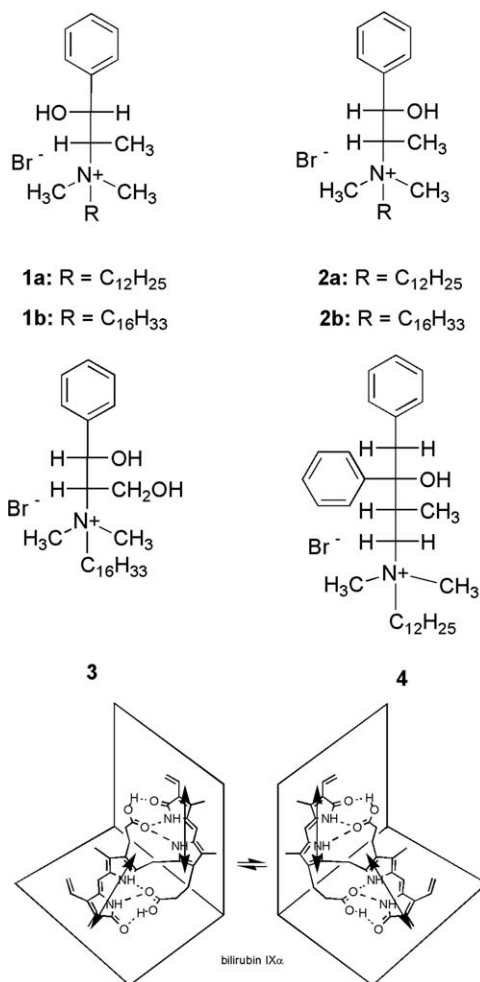
Contract grant sponsor: Dipartimento di Progettazione Molecolare.

\*Correspondence to: Giovanna Mancini, CNR, Istituto di Metodologie Chimiche, Sezione Meccanismi di Reazione and Dipartimento di Chimica, Università degli Studi di Roma "La Sapienza," P.le A Moro 5, 00185 Roma, Italy. E-mail: giovanna.mancini@uniroma1.it

Received for publication 19 May 2011; Accepted 11 August 2011

DOI: 10.1002/chir.21026

Published online 26 November 2011 in Wiley Online Library (wileyonlinelibrary.com).



**Scheme 1.** Chiral cationic surfactants 1–4 and probe of chirality bilirubin IX $\alpha$ .

Ultraviolet (UV) spectra were recorded on a Cary 300 UV-vis double beam spectrophotometer (Varian Pty, Mulgrave, AU).

Optical rotations were determined on a DIP370-JASCO digital polarimeter.

Conductivity experiments were performed on a Hanna conductimeter HI-9932, equipped with a thermostating apparatus.

### Preparation of Surfactants

**(–)-(1R,2S)-N-dodecyl-N,N-dimethylephedrinium bromide, 1a.** To a solution of 0.51 g (2.8 mmol) of (1R,2S)-(–)-N-methylephedrine in 4 ml of acetonitrile, 0.75 g (3.0 mmol) of 1-bromododecane were added. The reaction mixture was kept under reflux (~10 days) and monitored by TLC (CHCl<sub>3</sub>/MeOH = 80/20). After removal of the solvent under reduced pressure, the residue was washed with Et<sub>2</sub>O to give the crude product. Crystallization by methanol/ether yielded 0.48 g (40%) of a white powder (m.p. 104–106°C).

<sup>1</sup>H NMR,  $\delta$ (CDCl<sub>3</sub>) ppm: 0.844 (3H, t, –(CH<sub>2</sub>)<sub>11</sub>CH<sub>3</sub>); 1.136 (3H, d, –CHCH<sub>3</sub>); 1.220 (16H, m, –(CH<sub>2</sub>)<sub>8</sub>CH<sub>3</sub>); 1.300 (2H, m, –N(CH<sub>2</sub>)<sub>2</sub>CH<sub>2</sub>–); 1.668 (2H, m, –NCH<sub>2</sub>CH<sub>2</sub>–); 3.270 (3H, s, –NCH<sub>3</sub>); 3.3–3.5 (1H, m, –NCH<sub>2</sub>); 3.430 (3H, s, –NCH<sub>3</sub>); 3.584 (1H, m, –CH(CH<sub>3</sub>)–); 3.793 (1H, m, –NCH<sub>2</sub>); 5.482 (1H, d, –OH); 5.730 (1H, m, –CHOH–); 7.214 (1H, m, ar); 7.292 (2H, t, ar); 7.457 (2H, d, ar).

<sup>13</sup>C NMR,  $\delta$ (CDCl<sub>3</sub>) ppm: 7.26; 14.09; 22.65; 22.87; 26.37; 29.29; 29.38; 29.46; 29.57; 31.87; 49.48; 49.71; 64.26; 67.85; 72.85; 125.95; 127.57; 128.48; 141.17.  $\alpha_D$  = CH<sub>3</sub>OH, –11.2 (c 0.738, CH<sub>3</sub>OH)

Molar ellipticity (deg cm<sup>2</sup> dmol<sup>–1</sup>): +629 (267 nm); +792 (260 nm); +550 (255 nm); +283 (248 nm, shoulder); +133 (242 nm, shoulder); +54 (236 nm, shoulder).

**(–)-(1R,2S)-N-hexadecyl-N,N-dimethylephedrinium bromide, 1b.** 0.51 g (2.8 mmol) of (1R,2S)-(–)-N-methylephedrine were quaternized with 0.92 g (3.0 mmol) of 1-bromohexadecane according to the procedure described above for **1a**. Crystallization by methanol/ether yielded 0.61 g (45%) of a white powder (m.p. 117.0–118.5°C).

<sup>1</sup>H NMR,  $\delta$ (CDCl<sub>3</sub>) ppm: 0.838 (3H, t, –(CH<sub>2</sub>)<sub>11</sub>CH<sub>3</sub>); 1.130 (3H, d, –CHCH<sub>3</sub>); 1.215 (24H, m, –(CH<sub>2</sub>)<sub>12</sub>CH<sub>3</sub>); 1.297 (2H, m, –N(CH<sub>2</sub>)<sub>2</sub>CH<sub>2</sub>–); 1.681 (2H, m, –NCH<sub>2</sub>CH<sub>2</sub>–); 3.265 (3H, s, –NCH<sub>3</sub>); 3.40–3.51 (1H, m, –NCH<sub>2</sub>); 3.424 (3H, s, –NCH<sub>3</sub>); 3.565 (1H, m, –CHCH<sub>3</sub>); 3.770 (1H, m, –NCH<sub>2</sub>); 5.463 (1H, bs, –OH); 5.722 (1H, d, –CHOH–); 7.196 (1H, m, ar); 7.286 (2H, t, ar); 7.454 (2H, d, ar).

<sup>13</sup>C NMR,  $\delta$ (CDCl<sub>3</sub>) ppm: 7.27; 14.09; 22.65; 22.87; 26.37; 29.29; 29.32; 29.40; 29.48; 29.59; 29.62; 29.67; 31.89; 49.47; 49.71; 64.22; 67.82; 72.83; 125.96; 127.56; 128.48; 141.17.  $\alpha_D$  = –10.6 (c 1.28, CH<sub>3</sub>OH).

Molar ellipticity (CH<sub>3</sub>OH, deg cm<sup>2</sup> dmol<sup>–1</sup>): +633 (267 nm); +805 (260 nm); +566 (255 nm); +300 (248 nm, shoulder); +111 (241 nm, shoulder).

**(+)-(1S,2S)-N-dodecyl-N,N-dimethylpseudoephedrinium bromide, 2a.** 0.51 g (2.8 mmol) of (1S,2S)-(–)-N-methylpseudoephedrine were quaternized with 0.75 g (3.0 mmol) of 1-bromododecane. Purification by chromatography on silica gel in gradient of polarity (CHCl<sub>3</sub>/MeOH from 95/5 to 80/20) yielded 0.48 g (40%) of a yellow oil.

<sup>1</sup>H NMR,  $\delta$ (CDCl<sub>3</sub>) ppm: 0.836 (3H, t, –(CH<sub>2</sub>)<sub>11</sub>CH<sub>3</sub>); 1.120 (3H, d, –CHCH<sub>3</sub>); 1.212 (16H, m, –(CH<sub>2</sub>)<sub>8</sub>CH<sub>3</sub>); 1.261 (2H, m, –N(CH<sub>2</sub>)<sub>2</sub>CH<sub>2</sub>–); 1.684 (2H, m, –NCH<sub>2</sub>CH<sub>2</sub>–); 2.560 (1H, bs, OH); 3.223 (3H, s, –NCH<sub>3</sub>); 3.321 (1H, m, –NCH<sub>2</sub>); 3.374 (3H, s, –NCH<sub>3</sub>); 3.683 (1H, m, –CH(CH<sub>3</sub>)–); 3.800 (1H, m, –NCH<sub>2</sub>); 5.110 (1H, d, –CHOH–); 7.244 (1H, m, ar); 7.316 (2H, t, ar); 7.402 (2H, d, ar).

<sup>13</sup>C NMR,  $\delta$ (CD<sub>3</sub>OD) ppm: 13.35; 14.06; 22.62; 22.86; 26.32; 29.19; 29.27; 29.37; 29.44; 29.55; 31.84; 50.18; 51.19; 65.96; 71.38; 73.73; 127.44; 128.42; 128.85; 141.69.  $\alpha_D$  = +38.1 (c 1.92, CH<sub>3</sub>OH).

Molar ellipticity (CH<sub>3</sub>OH, deg cm<sup>2</sup> dmol<sup>–1</sup>): –178 (267 nm); –237 (262 nm); –160 (255 nm); –74 (250 nm, shoulder); –24 (244 nm, shoulder).

**(+)-(1S,2S)-N-hexadecyl-N,N-dimethylpseudoephedrinium bromide, 2b.** 0.51 g (2.8 mmol) of (–)-(1S,2S)-N-methylpseudoephedrine were quaternized with 0.92 g (3.0 mmol) of 1-bromohexadecane. Crystallization by methanol/ether yielded 0.54 g (40%) of a white powder (m.p. 90–92°C).

<sup>1</sup>H NMR,  $\delta$ (CDCl<sub>3</sub>) ppm: 0.836 (3H, t, –(CH<sub>2</sub>)<sub>11</sub>CH<sub>3</sub>); 1.029 (3H, d, –CHCH<sub>3</sub>); 1.214 (24H, m, –(CH<sub>2</sub>)<sub>12</sub>CH<sub>3</sub>); 1.262 (2H, m, –N(CH<sub>2</sub>)<sub>2</sub>CH<sub>2</sub>–); 1.690 (2H, m, –NCH<sub>2</sub>CH<sub>2</sub>–); 3.236 (3H, s, –NCH<sub>3</sub>); 3.30–3.42 (1H, m, –NCH<sub>2</sub>); 3.382 (3H, s, –NCH<sub>3</sub>); 3.712 (1H, m, –CH(CH<sub>3</sub>)–); 3.850 (1H, m, –NCH<sub>2</sub>); 5.085 (1H, d, –CHOH–); 7.269 (1H, m, ar); 7.310 (2H, t, ar); 7.391 (2H, d, ar).

<sup>13</sup>C NMR,  $\delta$ (CDCl<sub>3</sub>) ppm: 13.42; 14.07; 22.63; 22.90; 26.33; 29.21; 29.30; 29.38; 29.46; 29.58; 29.61; 29.65; 31.87; 50.19; 51.12; 65.91; 71.37; 73.78; 127.43; 128.43; 128.86; 141.67.  $\alpha_D$  = +35.1 (c 1.18, CH<sub>3</sub>OH).

Molar ellipticity (CH<sub>3</sub>OH, deg cm<sup>2</sup> dmol<sup>–1</sup>): –175 (267 nm); –222 (261 nm); –158 (255 nm); –74 (250 nm, shoulder); –30 (244 nm, shoulder).

**(+)-(1S,2S)-2-(dimethylamino)-1-phenylpropane-1,3-diol.** 50 ml (0.67 mol) of formaldehyde 40% w/v were added to 31.7 g (0.19 mol) of (+)-(1S,2S)-2-amino-1-phenylpropane-1,3-diol and cooled in an ice bath. After the addition of 25 ml (0.66 mol) of formic acid 99% under cooling, the mixture was heated to reflux for 24 h. After cooling, the addition of solid NaOH to the reaction mixture, saturated with NaCl, induced phase separation. The aqueous layer was extracted twice with 50 ml of CHCl<sub>3</sub>. The collected organic layers were washed with brine and dried on anhydrous Na<sub>2</sub>SO<sub>4</sub>. After removal of the solvent under reduced pressure, purification on silica gel (eluent, CH<sub>2</sub>Cl<sub>2</sub>/CH<sub>3</sub>OH 8:2) yielded 32 g (88%) of a white solid (m.p. 60–61°C).

<sup>1</sup>H NMR,  $\delta$ (CDCl<sub>3</sub>) ppm: 1.8 (2H, bs, 2OH); 2.50 (6H, s, 2CH<sub>3</sub>); 2.65 (1H, m, 1CH); 3.45 (2H, m, 1CH<sub>2</sub>); 4.4 (1H, d, 1CH); 7.4 (5H, m, Ar).  $\alpha_D$  = +45.9° (c 7.76, CHCl<sub>3</sub>).

**(+)-(1S,2S)-N-(1,3-dihydroxy-1-phenylpropan-2-yl)-N,N-dimethylhexadecan-1-ammonium bromide, 3.** 0.55 g (2.8 mmol) of (+)-(1S,2S)-2-(dimethylamino)-1-phenylpropane-1,3-diol were quaternized

with 0.92 g (3.0 mmol) of 1-bromohexadecane according to the procedure described above for **1a**. Crystallization by methanol/ether yielded 0.81 g (58%) of a white powder (m.p. 96–98°C).

<sup>1</sup>H NMR,  $\delta$ (CD<sub>3</sub>OD) ppm: 0.894 (3H, t, –(CH<sub>2</sub>)<sub>11</sub>CH<sub>3</sub>); 1.285 (24H, m, (CH<sub>2</sub>)<sub>12</sub>CH<sub>3</sub>); 1.406 (2H, m, N(CH<sub>2</sub>)<sub>2</sub>CH<sub>2</sub>–); 1.884 (2H, m, NCH<sub>2</sub>CH<sub>2</sub>–); 3.29–3.37 (m, 1H, –CH<sub>2</sub>OH); 3.377 (3H, s, NCH<sub>3</sub>); 3.462 (3H, s, NCH<sub>3</sub>); 3.680 (1H, m, –CH(CH<sub>2</sub>OH)); 3.70–3.98 (3H, m, –CH<sub>2</sub>OH + –NCH<sub>2</sub>); 5.373 (1H, d, –CHOH–); 7.33–7.47 (3H, m, ar); 7.500 (2H, d, ar).

<sup>13</sup>C NMR,  $\delta$ (CD<sub>3</sub>OD) ppm: 14.45; 23.72; 23.93; 27.54; 30.18; 30.45; 30.54; 30.64; 30.74; 30.77; 33.05; 51.81; 51.96; 58.93; 68.29; 72.79; 76.24; 128.51; 129.83; 129.92; 143.23.  $\alpha_D = +41.1^\circ$  (c 4.83, CH<sub>3</sub>OH).

Molar ellipticity (CH<sub>3</sub>OH, deg cm<sup>2</sup> dmol<sup>–1</sup>): –146 (267 nm); –186 (261 nm); –118 (255 nm); –49 (250 nm); –13 (244 nm, shoulder).

**(+)-(2R,3S)-N-(3-hydroxy-2-methyl-3,4-diphenylbutyl)-N,N-dimethyl-dodecan-1-ammonium bromide, 4.** 0.80 g (2.8 mmol) of Chiralol (99%) were quaternized with 0.74 g (3.0 mmol) of 1-bromododecane according to the procedure described above for **1a**. Crystallization by methanol/ether yielded 0.81 g (65%) of a white powder (m.p. 154–155°C).

<sup>1</sup>H NMR,  $\delta$ (CD<sub>3</sub>OD) ppm: 0.894 (3H, t, –(CH<sub>2</sub>)<sub>11</sub>CH<sub>3</sub>); 1.15 (3H, d, –CHCH<sub>3</sub>); 1.285 (18H, m, (CH<sub>2</sub>)<sub>9</sub>CH<sub>3</sub>); 1.730 (2H, m, NCH<sub>2</sub>CH<sub>2</sub>–); 2.311 (1H, m, –CHCH<sub>3</sub>); 2.651 (1H, dd, NCH<sub>2</sub>CHCH<sub>3</sub>); 2.960 (3H, s, NCH<sub>3</sub>); 2.974 (3H, s, NCH<sub>3</sub>); 3.186 (2H, m, –NCH<sub>2</sub>); 3.245 (1H, d, –CH<sub>2</sub>Ph); 3.467 (1H, d, –CH<sub>2</sub>Ph); 3.878 (1H, dd, NCH<sub>2</sub>CHCH<sub>3</sub>); 7.19–7.347 (6H, m, ar); 7.358 (2H, t, ar); 7.540 (2H, dd, ar).

<sup>13</sup>C NMR,  $\delta$ (CD<sub>3</sub>OD) ppm: 14.45; 18.58; 23.59; 23.72; 27.37; 30.19; 30.45; 30.54; 30.62; 30.73; 33.06; 37.97; 45.95; 51.22; 51.59; 65.98; 68.86; 78.54; 127.47; 127.86; 128.18; 128.79; 129.02; 132.17; 138.11; 144.43.  $\alpha_D = +4.77^\circ$  (c 4.28, CH<sub>3</sub>OH).

Molar ellipticity (CH<sub>3</sub>OH, deg cm<sup>2</sup> dmol<sup>–1</sup>): +275 (266 nm); +455 (260 nm); +433 (255 nm); +342 (251 nm, shoulder); +289 (248 nm, shoulder); +205 (243 nm, shoulder).

### Determination of Aggregative Parameters of Surfactants

Krafft point and Krafft temperature of surfactants **2–4** were measured by conductivity experiments according to a described procedure.<sup>31,32</sup> Note that the Krafft point is defined as the temperature at which the critical micelle concentration (CMC) versus temperature plot intersects the solubility versus temperature plot whereas the Krafft temperature is the temperature, above the cmc, at which the surfactant is completely soluble, hence is always higher than the Krafft point.<sup>33</sup> For the determination of Krafft point and Krafft temperature, a clear solution of surfactant in bidistilled water, at a concentration estimated above the cmc, was obtained by heating. The solution was kept at 4°C for 24 h to allow the precipitation of surfactant. When precipitation occurred, the conductivity of the solution at increasing temperature (at a rate of 0.5°C/min) was measured under stirring. In the plot conductivity versus temperature, the Krafft point was estimated by the first break whereas the Krafft temperature by the second one. When precipitation did not occur, the Krafft temperature was referred to as  $\leq 4^\circ\text{C}$  and not measured.

The cmc of surfactants **2–4** were measured by conductivity experiments.

**Sample preparation.** Micellar solutions were prepared by dissolving the proper amounts of surfactant in bidistilled water. Samples for UV–vis and CD investigations were prepared by adding the necessary volume ( $\mu\text{l}$ ) of 1 or 10 mM stock solutions of bilirubin in ultrapure dimethyl sulfoxide (DMSO) (dried on molecular sieves) to the aqueous surfactants solutions (<2%, v/v). Handling of bilirubin samples was performed in dim light. Spectra were recorded within 5 min since sample preparation in quartz cuvettes of different path length (0.1, 1 cm).

## RESULTS AND DISCUSSION

### Preparation and Characterization of Amphiphiles

All amphiphiles have been prepared by quaternization of the corresponding amines.

Chirality DOI 10.1002/chir

TABLE 1. Aggregation parameters of investigated surfactants

| Surfactant           | Krafft point (°C) | Krafft temperature (°C)  | cmc (mM)    |
|----------------------|-------------------|--------------------------|-------------|
| <b>1a</b>            | 15                | 30 (10 mM)<br>33 (20 mM) | 4.0 (25°C)  |
| <b>1b</b>            | 30                | 45                       | 0.4 (33°C)  |
| <b>2a</b>            | <4                | <4                       | 3.5 (25°C)  |
| <b>2b</b>            | 17                | 23                       | 0.21 (25°C) |
| <b>3</b>             | 44                | 52                       | 0.23 (50°C) |
| <b>4<sup>a</sup></b> | 42                | ~50 <sup>b</sup>         | –           |

<sup>a</sup>A clear break in the conductivity on increasing surfactant concentration and temperature was not observed.

<sup>b</sup>Temperature at which a 2 mM solution of **4** becomes clear.

The aggregation parameters, namely cmc, Krafft point, and temperature, were measured by conductivity experiments. Results are summarized in Table 1.

The cmc of surfactant **4** is very low (most probably  $<10^{-7}$  M) and could not be determined by conductivity measurements, being the values of conductivity in the range of concentration of cmc close to that of water.

### Chiral Recognition Experiments

The interaction between bilirubin and the aggregates formed by the chiral cationic surfactants **1–4** was studied by means of CD and UV–vis spectroscopies in water solution at the spontaneous pH (pH 6.0–6.5). The experiments were carried out on samples of 10 and 100  $\mu\text{M}$  bilirubin, at a surfactant concentration above the cmc to ensure the presence of micellar aggregates in solution.

CD and UV–vis experiments on 10 and 100  $\mu\text{M}$  bilirubin in aqueous solutions of 20 mM **1a** and 1 mM **1b** were carried out at 35 and 50°C, respectively (i.e., above the Krafft temperature of the surfactant solutions). The obtained spectra are reported in Figures 1 and 2. The CD spectra show a bisignate band in the region of absorbance of bilirubin. Interestingly, the intensity and the sign of the observed bands depend on the concentration conditions and on length of alkyl chain, as observed previously in aggregates formed by *N*-alkyl-*N,N*-dimethyl-*N*-(1-phenylethyl)ammonium bromides.<sup>30</sup> The CD spectrum of 10  $\mu\text{M}$  bilirubin in aggregates of **1a** shows a negative bisignate band of modest intensity, whereas the spectrum of 100  $\mu\text{M}$  bilirubin in aggregates of the same surfactant show a slightly more intense positive bisignate band (Fig. 1a). Both CD spectra were fully reproducible and, although modest, the intensity of the observed bands was of the same order of magnitude of that observed in the presence of other chiral selectors.<sup>27</sup>

On the other hand, both the CD spectra of 10 and 100  $\mu\text{M}$  bilirubin in aggregates of **1b** show a positive bisignate band (Fig. 2a) more intense than those observed in the experiments with **1a**. As reported previously, the occurrence of a bisignate band (an exciton couplet) for bilirubin, in a system lacking additional chromophores absorbing in the same region of the spectrum as bilirubin, can be reasonably ascribed to the deracemization of its racemic mixture.<sup>27,28</sup> Actually, it has to be pointed out that in the investigation of the diastereomeric interactions involving transparent chiral hosts and enantiomeric chromophores, a mirror-image relationship between the diastereomeric complexes is usually implicitly assumed and the possibility of differences in their CD

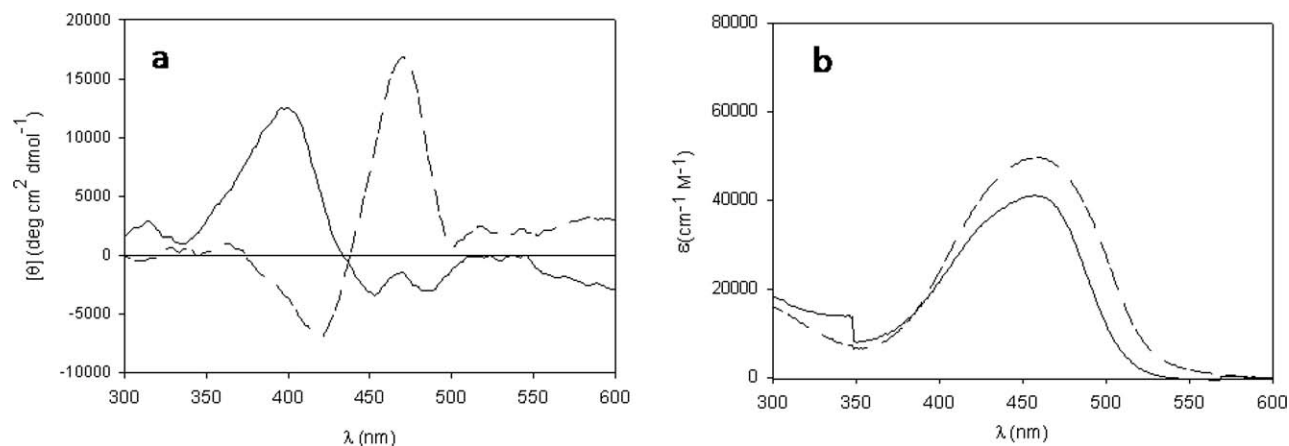


Fig. 1. CD (a) and UV-vis (b) spectra of 10  $\mu\text{M}$  (solid line) and 100  $\mu\text{M}$  (dashed line) bilirubin in aqueous 20 mM **1a**.

spectra are not considered. This approximation is generally feasible, although, if the enantiomeric excess is very modest, small chiroptical differences between the diastereomeric complexes come into play and may lead to non-vanishing CD spectra also for racemic mixtures. The shape of such CD spectra may either be “normal,” as expected for the enantiomers, if the CD spectra of diastereomers differ only in magnitude, or more complex, if the spectra are shifted relative to each other<sup>34</sup> (see below).

Given these considerations, it could be argued that the CD bands observed when bilirubin is in the presence of aggregates of **1a** result from the different intensity of the CD spectra of diastereomeric complexes rather than from a diastereomeric excess due to deracemization. However, the fact that the sign of the bands depends on the concentration condition suggests deracemization, although very modest.

As a matter of fact, a reversal of the Cotton effect sign of bilirubin can be observed, without an inversion of molecular chirality, in response to conformational changes, switching from values of the dihedral angle between the dipyrinone planes of bilirubin  $\theta < 140^\circ$  to  $\theta > 140^\circ$ . However, such a conformational change is accompanied by an absorbance increase of the higher energy transition of exciton splitting in the UV spectrum.<sup>35,36</sup> As the UV-vis spectra of bilirubin 10 and 100  $\mu\text{M}$  (Fig. 1b) do not show strong differences, featuring the two transitions of exciton splitting of similar intensity,

it is reasonable to expect similar conformations of the pigment at the two concentration conditions, with  $\theta \sim 100^\circ$ , as predicted by the exciton model.<sup>35,36</sup> Hence, it can be safely claimed that the inversion of the Cotton effect sign observed as a function of concentration of bilirubin in aggregates of **1a** is due to an inversion of molecular chirality. Evidently, the different concentration conditions induce either a different organization of the aggregates or a different site of binding of bilirubin, thus yielding an opposite enantioselection.

On the other hand, in aggregates of **1b** the inversion of the Cotton effect sign as a function of concentration of bilirubin was not observed (Fig. 2a). The analysis of UV-vis spectra in Figure 2b suggests a slightly more folded conformation of bilirubin in aggregates of **1b** with respect to **1a**.<sup>35,36</sup> The lower values of the molar extinction coefficient at the higher bilirubin concentration observed in Figure 2b are likely to be due to the aggregation of the pigment inside or at the surface of the micellar pseudophase because of the saturation of the micellar pseudophase (actually a marked Tyndall effect is observed at this concentration). Thus, the different intensity of the CD bands in Figure 2a can be reasonably ascribed to a similar extent of deracemization.

CD and UV-vis experiments on 10 and 100  $\mu\text{M}$  bilirubin in aqueous solutions of 50 mM **2a** and 10 mM **2b** were carried out at 25°C (Figs. 3 and 4). The CD spectra show bands whose intensity and shape depend on the length of the alkyl

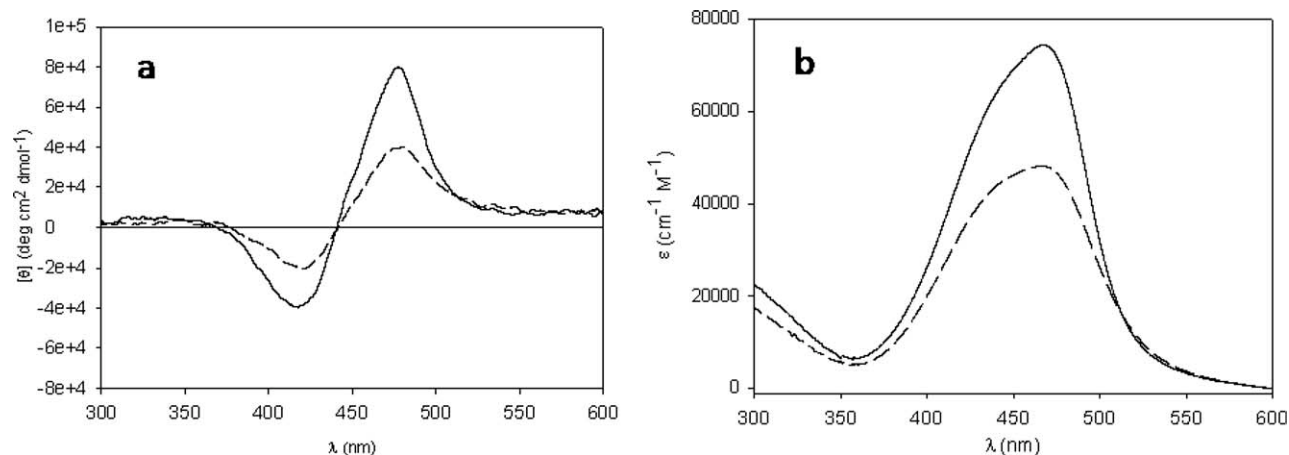


Fig. 2. CD (a) and UV-vis (b) spectra of 10  $\mu\text{M}$  (solid line) and 100  $\mu\text{M}$  (dashed line) bilirubin in aqueous 1 mM **1b**.

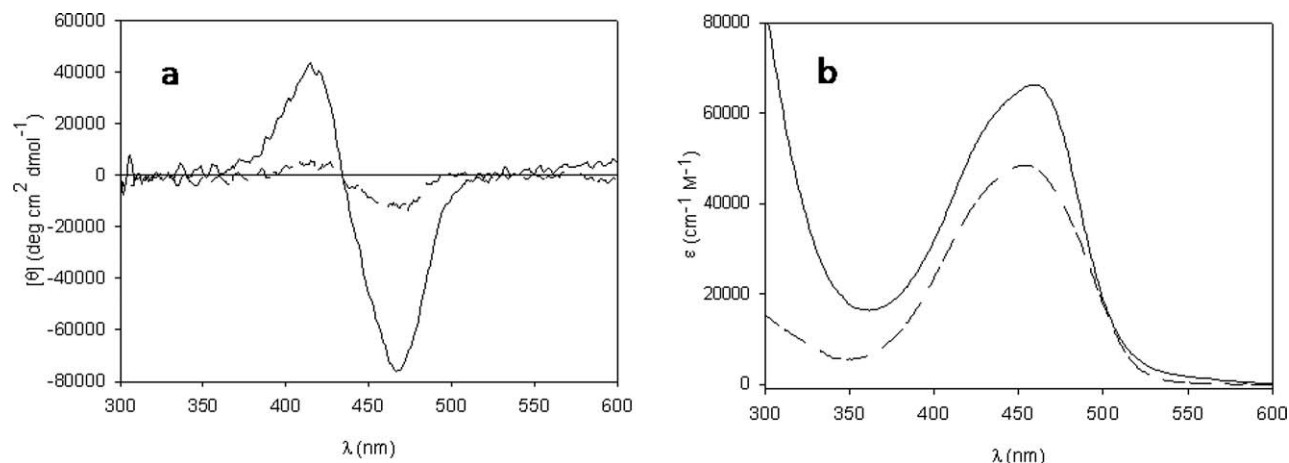


Fig. 3. CD (a) and UV-vis (b) spectra of 10  $\mu\text{M}$  (solid line) and 100  $\mu\text{M}$  (dashed line) bilirubin in aqueous 50 mM **2a**.

chain of surfactant and on bilirubin concentration. In the case of surfactant **2a** (Fig. 3a), the CD spectrum shows a negative bisignate band whose intensity strongly depends on bilirubin concentration, it being higher at the lower concentration of bilirubin (10  $\mu\text{M}$ ). Also in this case, the UV-vis spectra suggest a bilirubin folded conformation with  $\theta \sim 100^\circ$ <sup>35,36</sup> and the variation of the intensity of the CD band would suggest a different extent of deracemization modulated by the concentration conditions.

On the other hand, the CD spectra of bilirubin in the presence of surfactant **2b** (Fig. 4) show a more complex pattern and the shape of the CD bands strongly suggests the superimposition of two intense exciton couplets with inverted sign, similar magnitude and slightly different position.<sup>35</sup> Their origin can have different explanations: (i) the bilirubin enantiomers are bound to two different types of aggregates, probably induced by the addition of the chromophore itself; (ii) bilirubin is bound to different sites of the aggregate featuring opposite enantioselecting capabilities (e.g., the enantiomeric conformations of bilirubin could be, respectively, bound to the hydrophobic core of the micelles and to their polar region); (iii) bilirubin is bound to different sites of the aggregate that stabilize two nonenantiomeric conformations of bilirubin, with different dihedral angles, featuring inverted and slightly shifted CD spectra.

The first two hypotheses imply that different sites of binding (either different aggregates or regions within the same aggregate) can deracemize bilirubin in opposite direction, nearly at the same extent, and that the diastomeric complexes of the enantiopure aggregates with the enantiomers of bilirubin, i.e., M-bilirubin/**2b** and P-bilirubin/**2b**, feature a nonperfect mirror relationship of their CD spectra. Therefore, the results would indicate that the micellar aggregates are able to discriminate the enantiomers, without an overall deracemization of their mixture.

On the other hand, according to the third hypothesis the observed CD pattern does not imply any enantiodiscriminating process. However, the analysis of UV-vis spectra show the two exciton components of similar intensity which reasonably rules out the presence of nonenantiomeric bilirubin conformations featuring inverted CD spectra.<sup>35,36</sup>

To shed some light on the two discriminating sites and on the origin of the pattern of the observed CD bands, we carried out an annealing experiment, namely CD and UV experiment were carried on an aqueous solution of 10  $\mu\text{M}$  bilirubin and 10 mM **2b** heated to 50°C and then cooled back to 25°C. Noteworthy, by heating the sample, the complex CD band evolved irreversibly to a normal bisignate band (a negative couplet), as shown in Figure 5a where we reported the spectrum obtained at 25°C, before heating, and the spectrum

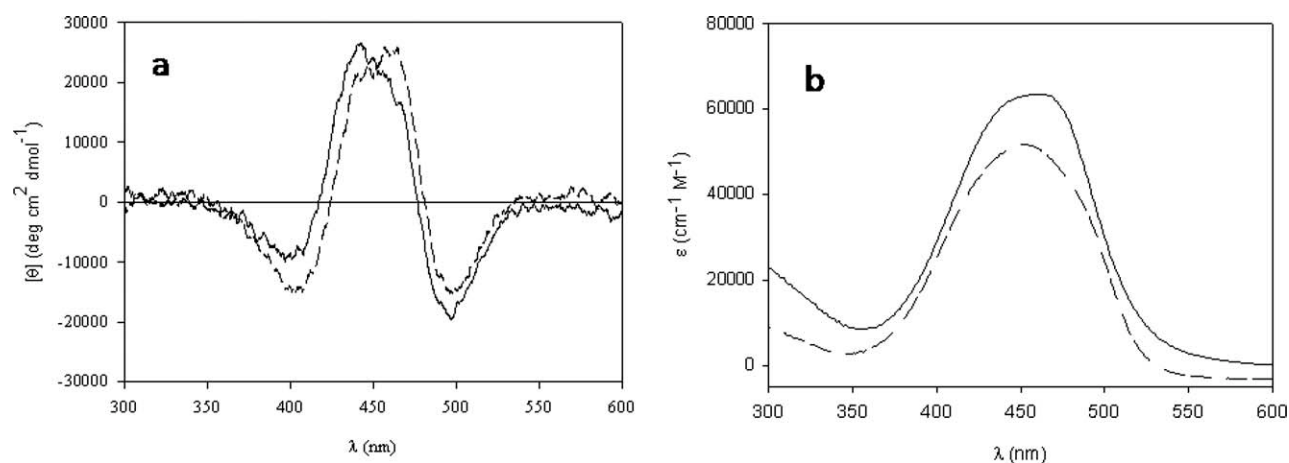


Fig. 4. CD (a) and UV-vis (b) spectra of 10  $\mu\text{M}$  (solid line) and 100  $\mu\text{M}$  (dashed line) bilirubin in aqueous 10 mM **2b**.

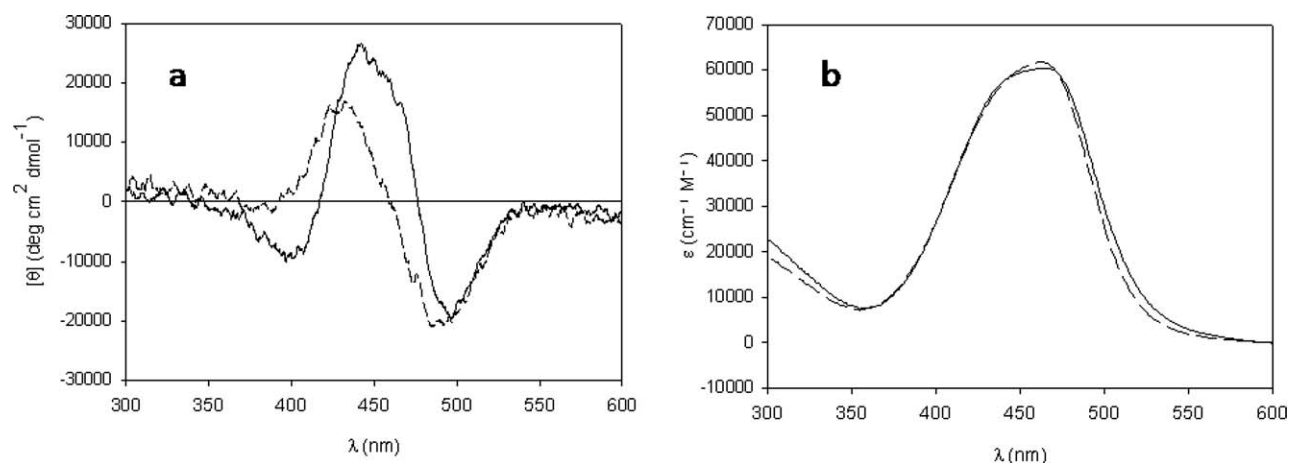


Fig. 5. CD (a) and UV-vis (b) spectra of 10  $\mu$ M bilirubin in aqueous 10 mM **2b** at 25°C (solid line) and 50°C (dashed line).

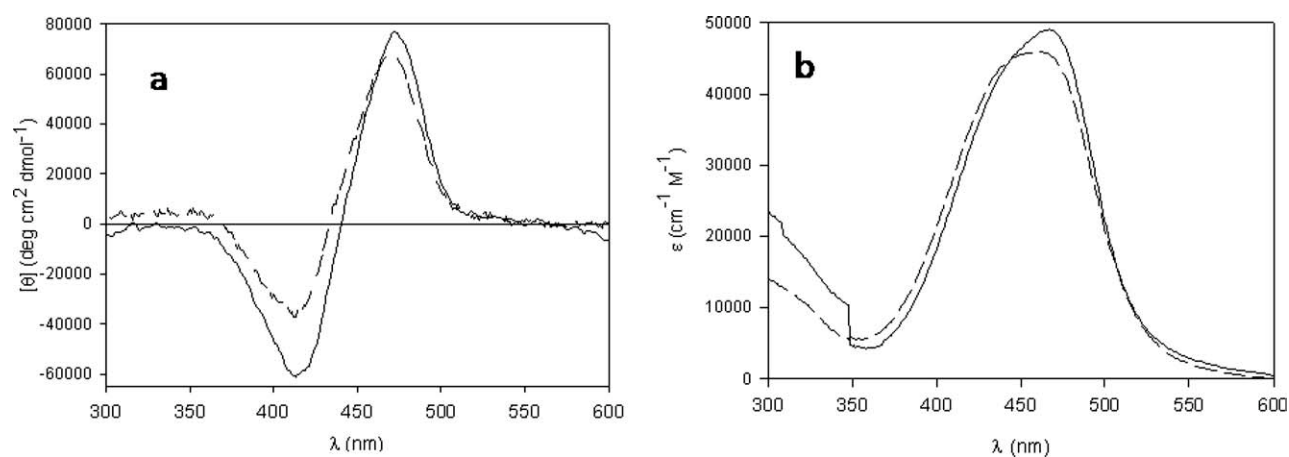


Fig. 6. CD (a) and UV-vis (b) spectra of 10  $\mu$ M (solid line) and 100  $\mu$ M (dashed line) bilirubin in aqueous 5 mM **3**.

obtained at 50°C. The spectrum obtained at 25°C after cooling back (not shown) was identical to that obtained at 50°C. On the other hand, the corresponding UV spectra obtained at 25 and 50°C show negligible differences (Fig. 5b). These results strongly suggest that in the aggregates of **2b**, under kinetic control, bilirubin is bound to different sites within the

aggregates with opposite enantioselecting capabilities, whereas under equilibrium conditions all the pigment features the same site of binding and in this case the overall result is deracemization.

Also in the experiments relative to the aggregates of **2a** and **2b**, the different behavior of bilirubin indicates a role of

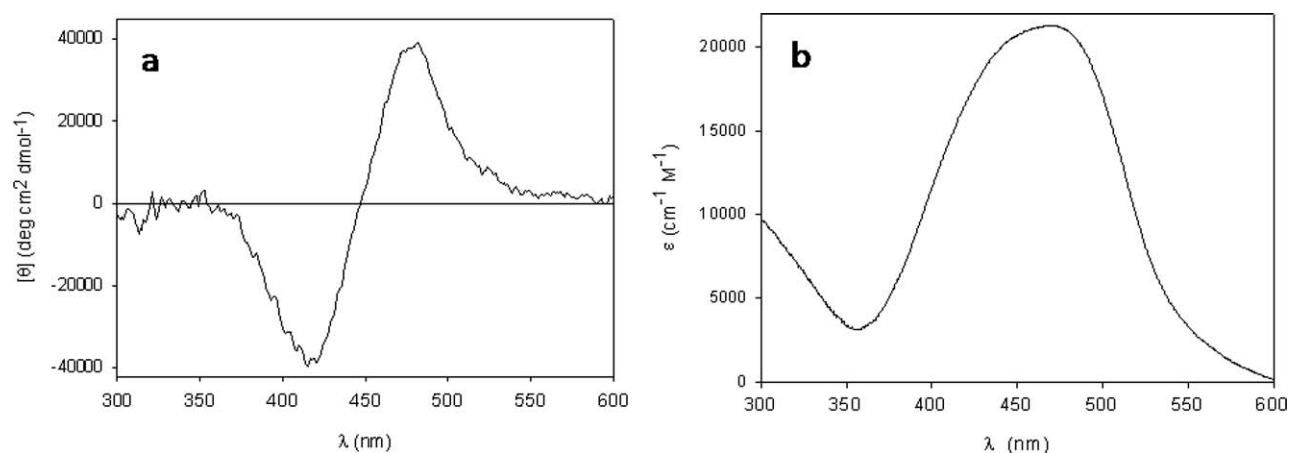


Fig. 7. CD (a) and UV-vis (b) spectra of 10  $\mu$ M bilirubin in aqueous 0.1 mM **4**.

the hydrophobic portion of the surfactant, and hence of the hydrophobic interactions, in the enantiodiscriminating processes.

The CD and UV-vis spectra of samples relative to different concentration of bilirubin in the presence of the aggregates of surfactant **3**, at 55°C, are reported in Figure 6. The CD spectra show an intense positive bisignate band likely suggesting a high extent of deracemization. The intensity of the band is almost independent from the surfactant/bilirubin ratio. However, an analysis of the UV-vis spectra shows that the shape of the UV band depends on the concentration conditions, thus suggesting different conformations of bilirubin at the different surfactant/bilirubin ratios. In particular, at 10 μM bilirubin (surfactant/bilirubin ratio 500:1), the lower energy transition of exciton splitting is more intense, thus suggesting a slightly higher value of the dihedral angle between the dipyrinone chromophores. This would correspond to a smaller molar ellipticity as calculated by the exciton coupling theory.<sup>36</sup> Thus, the almost equal intensity observed in the CD spectra at the two different concentrations of bilirubin would be associated with a different extent of deracemization (i.e., higher at lower bilirubin concentration).

The CD and UV-vis spectra of samples relative to 10 μM bilirubin in the presence of the aggregates of surfactant **4**, at 52°C, are reported in Figure 7. The CD spectrum shows an intense positive bisignate band corresponding to a relatively high extent of deracemization, the UV-vis spectrum indicating a conformation with  $\theta \sim 100^\circ$ .

It is worth of note that only a modest bleaching of the pigment was observed when the experiments were carried out at high temperature, thus indicating that the aggregates protect bilirubin from degradation.<sup>26,35</sup>

## CONCLUSIONS

We have investigated by CD experiments the deracemization of bilirubin in chiral micellar aggregates with the aim of exploring the expression of chirality within the aggregates. The chiral information of the monomer can be translated into opposite enantiodiscriminating capability of the aggregates as a function of bilirubin concentration and of the length of the alkyl chain of the surfactant, demonstrating the fundamental role of hydrophobic interactions in the transfer of the chiral information from the monomers to the aggregates. It is possible that the observed deracemization processes also result from the interaction of functional groups of bilirubin with the functional groups of the surfactants. Actually an interaction with the head group functional groups could be responsible for the kinetic trapping observed in aggregates of **2b**; however, as deracemization is observed only in aggregating condition, it is clear that these interactions are mediated by aggregation.

Interestingly, in some cases the deracemization of bilirubin in chiral surfactant aggregates was observed at high temperature, where chiral recognition phenomena are, in general, less efficient due to less tight interactions between the interacting species.

## ACKNOWLEDGMENTS

The authors thank Prof. David A. Lightner for helpful discussion. This work was carried out in the frame of CM0703 "Systems Chemistry" COST Action.

## LITERATURE CITED

- Walde P, Blöchliger E, Morigaki K. Circular dichroic properties of phosphatidylcholine micelles. *Langmuir* 1999;15:2346–2350.
- Dobashi A, Hamada M. Molecular recognition with micellar and micelle-like aggregates in aqueous media. *J Chromatogr A* 1997;780:179–189.
- Tickle D, George A, Jennings K, Camilleri P, Kirby AJ. A study of the structure and chiral selectivity of micelles of two isomeric D-glucopyranoside-based surfactants. *J Chem Soc Perkin Trans 2* 1998:467–474.
- Ceccacci F, Mancini G, Sferazza A, Villani C. pH variation as the switch for chiral recognition in a biomembrane model. *J Am Chem Soc* 2005;127:13762–13763.
- Ceccacci F, Giansanti L, Mancini G, Mencarelli P, Sorrenti A. Discrimination of the enantiomers of new biphenylic derivatives in chiral micellar aggregates. *New J Chem* 2007;31:86–92.
- Alzalamira A, Ceccacci F, Monti D, Levi Mortera S, Mancini G, Sorrenti A, Venanzi M, Villani C. Discrimination of the enantiomers of biphenylic derivatives in micellar aggregates formed by chiral amidic surfactants. *Tetrahedron Asymmetry* 2007;18:1868–1876.
- Borocci S, Erba M, Mancini G, Scipioni A. Deracemization of an axially chiral biphenylic structure in chiral micellar aggregates. *Langmuir* 1998;14:1960–1962.
- Bella J, Borocci S, Mancini G. Recognition in organized aggregates formed by a chiral amidic surfactant. *Langmuir* 1999;15:8025–8031.
- Borocci S, Ceccacci F, Galantini L, Mancini G, Monti D, Scipioni A, Venanzi M. Deracemization of an axially chiral biphenylic derivative as a tool for investigating chiral recognition in self-assemblies. *Chirality* 2003;15:441–447.
- Nakagawa H, Onoda M, Masuoka Y, Yamada K-I. Effect of phosphatidylcholine vesicle size on chirality induction and chiral discrimination. *Chirality* 2006;18:212–216.
- Nakagawa H, Kobori Y, Yoshida M, Yamada K-I. Chiral recognition by single bilayered phosphatidylcholine vesicles using [5]thiaheterohelicene as a probe. *Chem Commun* 2001:2692–2693.
- Cruciani O, Borocci S, Lamanna R, Mancini G, Segre AL. Chiral recognition of dipeptides in phosphatidylcholine aggregates. *Tetrahedron Asymmetry* 2006;17:2731–2737.
- Arnett EM, Gold JM. Chiral aggregation phenomena. 4. A search for stereospecific interactions between highly purified enantiomeric and racemic dipalmitoyl phosphatidylcholines and other chiral surfactants in monolayers, vesicles, and gels. *J Am Chem Soc* 1982;104:636–639.
- Lalitha S, Kumar AS, Stine KJ, Covey DF. Chirality in membranes: first evidence that enantioselective interactions between cholesterol and cell membrane lipids can be a determinant of membrane physical properties. *J Supramol Chem* 2001;1:53–61.
- Pathirana S, Neely WC, Myers LJ, Vodyanov V. Chiral recognition of odorants (+)- and (-)-carvone by phospholipid monolayers. *J Am Chem Soc* 1992;114:1404–1405.
- Alakoskela J-M, Sabatini K, Jiang X, Laitala V, Covey DF, Kinnunen PKJ. Enantiospecific interactions between cholesterol and phospholipids. *Langmuir* 2008;24:830–836.
- Sorrenti A, Diociaiuti M, Corvaglia V, Chistolini P, Mancini G. Chiral recognition of dipeptides in Langmuir monolayers. *Tetrahedron Asymmetry* 2009;20:2737–2741.
- Fuhrhop JH, Schnieder P, Rosenberg J, Boekema E. The chiral bilayer effect stabilizes micellar fibers. *J Am Chem Soc* 1987;109:3387–3390.
- Uragami M, Miyake Y, Regen SL. Influence of headgroup chirality on the mixing behavior of phosphatidylglycerol mimics in fluid bilayers. *Langmuir* 2000;16:3491–3496.
- Andreani R, Bombelli C, Borocci S, Lah J, Mancini G, Mencarelli P, Vesnaver G, Villani C. New biphenylic derivatives: synthesis, characterisation and enantiodiscrimination in chiral aggregates. *Tetrahedron Asymmetry* 2004;15:987–994.
- Bombelli C, Borocci S, Lupi F, Mancini G, Mannina L, Segre AL, Viel S. Chiral recognition of dipeptides in a biomembrane model. *J Am Chem Soc* 2004;126:13354–13362; and references therein.
- Navon G, Frank S, Kaplan D. A nuclear magnetic resonance study of the conformation and the interconversion between the enantiomeric conformers of bilirubin and mesobilirubin in solution. *J Chem Soc Perkin Trans2* 1984:1145–1149.

23. Blauer G. Optical activity of bile pigments. *Isr J Chem* 1983;23:201–209.
24. Blauer G. Complexes of bilirubin with proteins. *Biochim Biophys Acta* 1986;884:602–604.
25. Lightner DA, Wijekoon WMD, Zhang MH. Understanding bilirubin conformation and binding. Circular dichroism of human serum albumin complexes with bilirubin and its esters. *J Biol Chem* 1988;263:16669–16676.
26. McDonagh AF. Bile Pigments: bilatrienes and 5,15-biladienes. In: Dolphin D, editor. *The porphyrins*, Vol. 6. New York: Academic Press; 1979. p 293–491.
27. Lightner DA, Gawronski JK, Wijekoon WMD. Complementarity and chiral recognition: enantioselective complexation of bilirubin. *J Am Chem Soc* 1987;109:6354–6362.
28. Lightner DA, Gawronski JK, Gawronska K. Conformational enantiomerism in bilirubin. Selection by cyclodextrins. *J Am Chem Soc* 1985;107:2456–2461.
29. Ceccacci F, Giansanti L, Levi Mortera S, Mancini G, Sorrenti A, Villani C. Enantiodiscrimination of bilirubin-IX $\alpha$  enantiomers in biomembrane models: has chirality a role in bilirubin toxicity? *Biorg Chem* 2008;36:252–254.
30. Bombelli C, Bernardini C, Elemento G, Mancini G, Sorrenti A, Villani C. Concentration as the switch for chiral recognition in biomembrane models. *J Am Chem Soc* 2008;130:2732–2733.
31. Filipović-Vinceković N, Babić-Ivančić V, Šmit I. Interactions in aqueous systems containing sodium cholate/calcium chloride mixtures. *J Colloid Interface Sci* 1996;177:646–657.
32. Bales BL, Benrraou M, Zana R. Krafft temperature and micelle ionization of aqueous solutions of cesium dodecyl sulfate. *J Phys Chem B* 2002;106:9033–9035.
33. Rubinch DN, Holland PM, editors. *Surfactant science series—cationic surfactants, physical chemistry*, Vol.37. New York and Basel: Marcel Dekker; 1991. p. 171–177.
34. Krois D, Lehner H. Induced circular dichroism and chiral discrimination of racemates revisited: bilirubins as illustrative examples. *J Chem Soc Perkin Trans 2* 1995;489–494.
35. Trull FR, Person RV, Lightner DA. Conformational analysis of symmetric bilirubin analogs with varying length alkanolic acids. Enantioselectivity by human serum albumin. *J Chem Soc Perkin Trans 2* 1997;1241–1250.
36. Person RV, Peterson BR, Lightner DA. Bilirubin conformational analysis and circular dichroism. *J Am Chem Soc* 1994;116:42–59.